We are IntechOpen, the world's leading publisher of Open Access books Built by scientists, for scientists

4,800
Open access books available

122,000
International authors and editors

135M
Downloads

Our authors are among the

154
Countries delivered to

TOP 1%
most cited scientists

12.2%
Contributors from top 500 universities

CLARIVATE ANALYTICS BOOK CITATION INDEX INDEXED

WEB OF SCIENCE™

Selection of our books indexed in the Book Citation Index in Web of Science™ Core Collection (BKCI)

Interested in publishing with us?
Contact book.department@intechopen.com

Numbers displayed above are based on latest data collected.
For more information visit www.intechopen.com

8

Photonic Crystal Fibre Interferometer for Humidity Sensing

Jinesh Mathew, Yuliya Semenova and Gerald Farrell
Photonics Research Centre, Dublin Institute of Technology
Ireland

1. Introduction

Photonic crystal fibres (PCFs), which are also called microstructured optical fibres or holey fibres, have been extensively investigated and have considerably altered the traditional fibre optics since they appeared in the mid 1990s [Knight et al., 1996; Knight, 2003; Russell, 2003]. PCFs have a periodic array of microholes that run along the entire fibre length. They typically have two kinds of cross sections: an air–silica cladding surrounding a solid silica core or an air–silica cladding surrounding a hollow core. The light-guiding mechanism of the former is provided by means of a modified total internal reflection (index guiding), while the light-guiding mechanism of the latter is based on the photonic band gap effect (PBG guiding). The number, size, shape, and the separation between the air-holes as well as the air-hole arrangement are what confer PCFs unique guiding mechanism and modal properties [Russell, 2006]. This gives PCF many unique properties such as single mode operation over a wide wavelength range [Birks et al., 1997], very large mode area [Knight et al., 1998], and unusual dispersion [Renversez et al., 2003]. Because of their freedom in design and novel wave-guiding properties, PCFs have been used for a number of novel fibre-optic devices and fibre-sensing applications that are difficult to be realized by the use of conventional fibres.

While optical interferometers offer high resolution in metrology applications, the fibre optic technology additionally offers many degrees of freedom and some advantages such as stability, compactness, and absence of moving parts for the construction of interferometers. The two commonly followed approaches to build fibre optic interferometer are: two arm interferometer and modal interferometer. Two- arm interferometer involves splitting and recombining two monochromatic optical beams that propagate in different fibres which requires several meters of optical fibre and one or two couplers. Modal interferometer exploits the relative phase displacement between two modes of the fibre. In modal interferometers compared to their two-arm counterparts the susceptibility to environmental fluctuations is reduced because the modes propagate in the same path or fibre. Recently the unique properties of the photonic crystal fibre have attracted the sensor community. Design of PCF based interferometers in particular is interesting owing to their proven high sensitivity and wide range of applications. Photonic crystal fibre based modal interferometers include PCFs in a fibre loop mirror [Zhao et al., 2004], interferometer built with long period gratings [Lim et al., 2004], interferometers built with tapered PCFs

[Monzón-Hernández et al., 2008], and interferometers fabricated via micro-hole collapse [Choi et al., 2007; Villatoro et al., 2007a]. The latter technique is really simple since it only involves cleaving and splicing. The different configurations reported so far are a PCF with two collapsed regions separated by a few centimetres [Choi et al., 2007], a short section of a PCF longitudinally sandwiched between standard single mode fibres by fusion splicing (transmission type) [Villatoro et al., 2007] and a stub of PCF with cleaved end fusion spliced at the distal end of a single mode fibre (reflection type) [Jha et al., 2008]. The advantage of the last two configurations is that the modal properties of the PCF are exploited but the interrogation is carried out with conventional optical fibres, thus leading to more cost-effective interferometers. The interferometer with the latter configuration is demonstrated in this chapter as a relative humidity or dew sensor. The sensor presented has the unique advantages such as it does not require any special coatings to measure humidity. Also since the sensor head is made of single material (silica) it can be used in harsh and high-temperature environments to monitor humidity.

In section 2 of the chapter the operating principle of a reflection type photonic crystal fibre interferometer (PCFI), its fabrication and the dependence of the interferometer's fringe spacing on the length of the PCF are presented. Section 3 explains the water vapor adsorption/desorption phenomena on a silica surface, the working principle of a relative humidity sensor based on PCF interferometer and the humidity response of the PCF interferometer. Section 4 demonstrates the use of the PCFI as a dew sensor. The section presents the basic sensing principle of the dew sensor, the temperature dependence and the dew response of the PCF interferometer. A dew point hygrometer using PCF interferometer is also proposed in this section.

2. Photonic crystal fibre interferometer

Photonic crystal fibre interferometers based on micro-hole collapse have attained great importance in recent times due to the simple fabrication process involved and excellent sensing performance [Villatoro et al., 2007, 2009a, 2009b]. A reflection-type PCFI consists of a stub of PCF fusion spliced at the distal end of a single mode fibre [Mathew et al., 2010]. The key element of the device is the hole collapsed region close to the splice point. Some advantages of the PCF interferometers fabricated using microhole collapse are that since interferometers are fabricated by fusion splicing the splice is highly stable even at high temperatures and also its characteristics will not degrade over time.

2.1 PCFI working principle

In a PCFI the excitation and recombination of modes can be carried out by the hole collapsed region of the PCF [Choi et al., 2007; Villatoro et al., 2007]. A microscopic image of the PCFI and a schematic of the excitation and recombination of modes in the PCFI are shown in Fig. 1. The fundamental SMF mode begins to diffract when it enters the collapsed section of the PCF. Because of diffraction, the mode broadens; depending on the modal characteristics of the PCF and the hole collapsed region, the power in the input beam can be coupled to the fundamental core mode and to higher order core modes [Villatoro et al., 2007, 2009b; Barrera et al., 2010] or to cladding modes [Cárdenas-Sevilla et al., 2011; Choi et al., 2007; Jha et al., 2008] of the PCF. The modes propagate through the PCF until they reach the cleaved end from where they are reflected. Since the modes propagate at different phase

velocities, thus in a certain length of PCF the modes accumulate a differential phase shift. Therefore constructive or destructive interference occurs along the length of PCF. The phase velocities and phase difference are also wavelength dependent; therefore the optical power reflected by the device will be a maximum at certain wavelengths and minimum at others [Villatoro et al., 2009b]. When the reflected modes re-enter the collapsed region they will further diffract and because the mode field of the SMF is smaller, the core acts as a spatial filter and picks up only a part of the resultant intensity distribution of the interference pattern in the PCF.

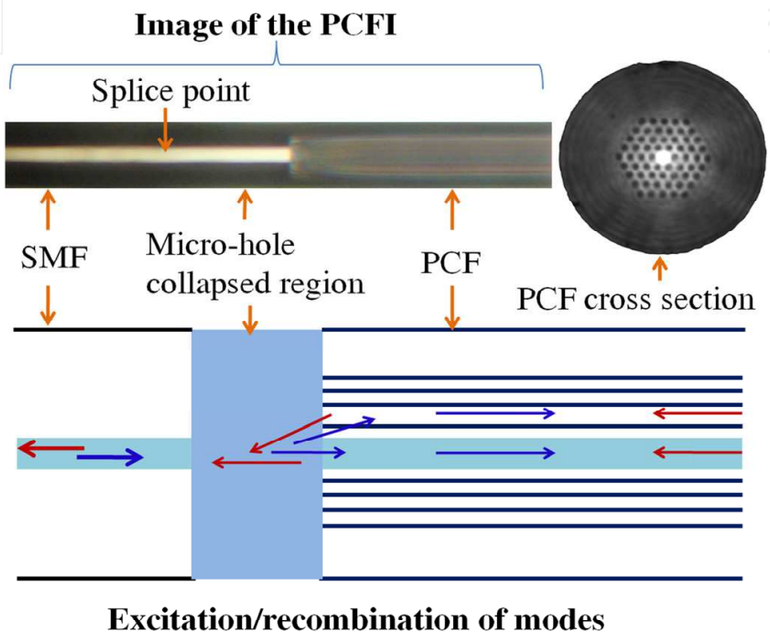

Fig. 1. Microscope image of the PCFI (upper) & a schematic of the excitation/recombination of modes in the hole collapsed region (lower).

A regular interference pattern in the reflection spectrum of the PCFI suggests that only two modes are interfering in the device. In our reported work [Mathew et al., 2010] on a PCFI using LMA 10 fibre, based on the fact that higher order modes can exist in the core of a PCF with a short length [Káčik et al., 2004; Uranus et al., 2010], the interfering modes in the PCF are considered as two core modes. However in a later experiment, which involved varying the refractive index surrounding the cladding of a PCFI, good ambient refractive index sensitivity is observed for a PCFI fabricated using the same LMA 10 fibre. This suggests that the interfering modes are a core mode and a cladding mode of the PCF, a conclusion that is supported by [Choi et al., 2007; Cárdenas-Sevilla et al., 2011] for an LMA10 fibre. Thus considering a core mode and a cladding mode as the interfering modes of the PCFI and designating the effective refractive indexes of the core mode as n_c and cladding mode as n_{cl}, the accumulated phase difference is $2\pi\Delta n(2L)/\lambda$, where $\Delta n=n_c-n_{cl}$, λ the wavelength of the optical source, and L the physical length of the PCFI [Villatoro et al., 2009a]. The power reflection spectrum of this interferometer will be proportional to $\cos(4\pi\Delta nL/\lambda)$. The wavelengths at which the reflection spectrum shows maxima are those that satisfy the condition $4\pi\Delta nL/\lambda=2m\pi$, with m being an integer. This means that a periodic constructive

interference occurs when $\lambda m = (2\Delta nL/m)$. If some external stimulus changes Δn (while L is fixed) the position of each interference peak will change, a principle which allows the device to be used for sensing.

2.2 PCFI fabrication

Fusion splicing of the PCF to the SMF is undertaken using the electric arc discharge of a conventional arc fusion splicer. During the splicing process the voids of the PCF collapse through surface tension within a microscopic region close to the splice point. In fabricating such an interferometer, one critical condition for good sensor performance is achieving a regular interference pattern and good interference fringe visibility. The visibility of the interferometer depends on the power in the excited modes, which in turn depends on the length of the collapsed region [Barrera et al., 2010]. However a long collapsed region length causes activation of many cladding modes and therefore degrades the sinusoidal nature of the interference patterns and furthermore increases the splice loss. Therefore for an improved sensor performance, only one cladding mode is preferred due to its simple interference with the core mode. The collapsed region length can be controlled by the arc power and duration [Barrera et al., 2010]. In our experiments, PCF (LMA10, NKT Photonics) designed for an endless single-mode operation was used. It has four layers of air holes arranged in a hexagonal pattern around a solid silica core. The light guidance mechanism in such a fibre is by means of modified total internal reflection. The dimensions of the LMA-10 PCF simplify alignment and splicing with the SMF with a standard splicing machine and minimize the loss due to mode field diameter mismatch compared to other PCFs. For the interferometer fabricated in our study the total length of the collapsed region was 200 μm. After fusion splicing, the PCF was cleaved using a standard fibre cleaving machine so that the end surface of the PCF acts as a reflecting surface.

2.3 PCFI fringe spacing vs length of PCF

Initially to investigate the influence of the length of the PCFI on the fringe spacing thirteen PCFIs were fabricated with lengths ranging from 3.5 mm to circa 100 mm. As an example Fig. 2 shows the measured reflection spectra of three PCFIs in the 1500-1600 nm wavelength range with lengths of 92, 10.5 and 3.5 mm. The reflection spectra of the interferometers exhibit regular interference patterns with a period or fringe spacing inversely proportional to the length of the PCF section. A modulation of the expected sinusoidal pattern is observed for the spectra shown in Fig. 2, which might be due to the excitation of more than one cladding mode or possibly due to the polarization dependence of the intermodal interference [Bock et al., 2009]. Fig. 3 shows the measured fringe spacing or periods of the fabricated PCFIs as a function of length of the PCF section. The measured periods agree well with the expected ones for a two-mode interferometer given by the expression $P \approx \lambda^2/(2\Delta nL)$. The value of Δn obtained based on the experimental data is $\sim 4.2 \times 10^{-3}$.

3. Relative humidity sensor based on PCFI

Humidity refers to the water vapour content in air or other gases and its measurements can be stated in a variety of terms and units. The three commonly used terms are absolute humidity, relative humidity (RH) and dew point. Absolute humidity is the ratio of the mass of water vapour to the volume of air or gas. It is commonly expressed in grams per cubic

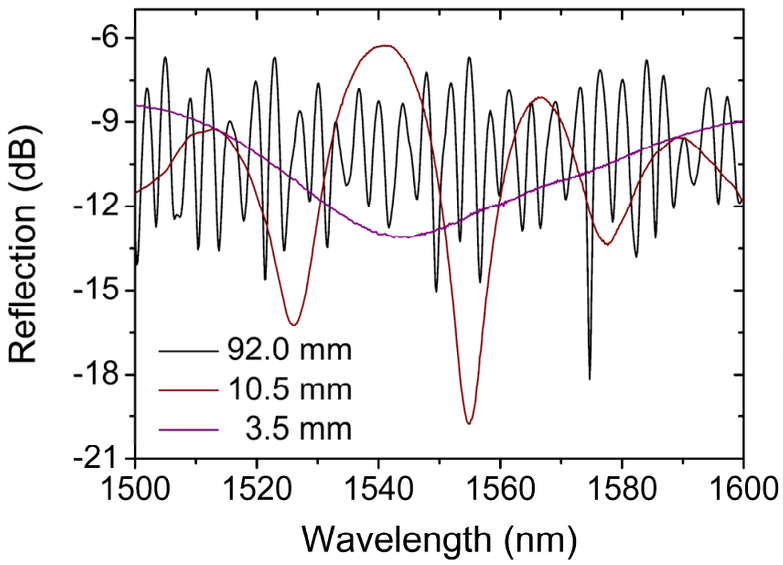

Fig. 2. The reflection spectra of interferometers with L = 92 mm, 10.5 mm and 3.5 mm in the wavelength range of 1500-1600 nm.

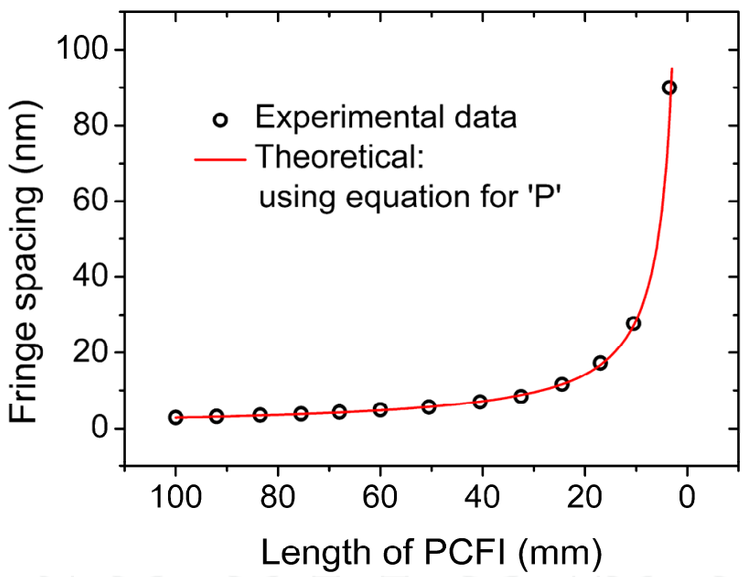

Fig. 3. The fringe spacing as a function of length of PCF observed for a reflection type interferometer.

meter. Dew point, expressed in °C or °F, is the temperature and pressure at which a gas begins to condense into a liquid. The ratio of the percentage of water vapour present in air at a particular temperature and pressure to the maximum amount of water vapour the air can hold at that temperature and pressure is the relative humidity.

The measurement of humidity is required in a range of areas, including meteorological services, the chemical and food processing industries, civil engineering, air-conditioning, horticulture and electronic processing. Compared with their conventional electronic

counterparts, optical fibre humidity sensors offer specific advantages, such as small size and weight, immunity to electromagnetic interference, corrosion resistance and remote operation. A wide range of optical fibre humidity sensors have been reported in the literature. Most of these fibre optic humidity sensors work on the basis of a hygroscopic material coated over the optical fibre to modulate the light propagating through the fibre [Yeo et al., 2008; Mathew et al. 2007, 2011]. A polymer optical fibre has been adapted for humidity sensing [Zhang et al., 2010] without the use of a hygroscopic coating but the fibre is highly temperature dependent and is not suitable for high-temperature applications. An all-glass fibre-optic relative humidity sensor which does not require any special coatings to measure humidity using a reflection-type two-mode photonic crystal fibre interferometer is presented in this section. The spectrum of it exhibits good sensitivity to humidity variations.

3.1 Operating principle of the sensor

An untreated silica PCF is used for the fabrication of the PCFI, its surface is hydrophilic and there fore the adsorption of water vapour on the surface occurs when it is exposed to humid air. Two types of water-vapour adsorption mechanisms occur in sequence at the SiO_2-air interface. The chemisorption of water vapour first modifies the SiO_2 surface, resulting in a surface with silanol groups (Si-OH). The second type of adsorption, physisorption, occurs on these silanol groups. A schematic illustration of the water-vapour adsorption is given in Fig. 4. At room temperature the physisorption is a reversible function of the relative humidity of the surrounding air, while the chemisorption appears to be irreversible [Voorthuyzen et al., 1987]. So in the succeeding discussion only the physisorption is considered. Awakuni and Calderwood [Awakuni & Calderwood, 1972] investigated the adsorption of water vapour on the SiO_2 surface. They measured the amount of adsorbed water as a function of the partial vapour pressure at a constant temperature. It appeared that this so-called adsorption isotherm can be described very well by the BET (Brunauer-Emmett- Teller) adsorption theory [Brunauer et al., 1938].

The evolution of adsorbed water layer structure on silicon oxide at room temperature is demonstrated by David and Seong in [David & Seong, 2005]. They determined the molecular configuration of water adsorbed on a hydrophilic silicon oxide surface at room temperature as a function of relative humidity using attenuated total reflection (ATR)-infrared spectroscopy. A completely hydrogen-bonded ice like network of water grows up as the relative humidity increases from 0 to 30%. In the relative humidity range of 30-60%, the liquid water structure starts appearing while the ice like structure continues growing to saturation. Above 60% relative humidity, the liquid water configuration grows on top of the ice like layer. This structural evolution indicates that the outermost layer of the adsorbed water molecules undergoes transitions in equilibrium behaviour as humidity varies. Also it was shown from the adsorption isotherm that the thickness of the adsorbed layer at room temperature starts increasing exponentially above 60% RH.

Tiefenthaler and Lukosz [Tiefenthaler & Lukosz, 1985] have shown that adsorption and desorption of water vapour by the surface of a waveguide changes the effective refractive index (RI) of the guided modes, in their case for a humidity sensor based on an integrated optical grating coupler. In the case of a PCFI a similar adsorption of water vapour changes the effective refractive index (n_{cl}) of the interfering cladding mode propagating in the PCF. Since this adsorption/physisorption is a reversible process, a modulation of the n_{cl} occurs

with respect to the ambient humidity values which in turn change the position of the interference pattern accordingly. An increase in humidity causes the shift of the interference pattern of a PCFI toward longer wavelengths and the value of this interference peak shift is exponential with respect to relative humidity [Mathew, 2010]. This shift of the interference peak is mainly due to the adsorption and desorption of H_2O molecules along the surface of holes within the PCF, at the interface between air and silica glass. Since the whole device is exposed to humidity the adsorption and desorption of water vapour on the PCF outer surface and on the end face also contribute to the shift of the interference pattern. But considering the field distribution of the interfering cladding mode shown in [Cárdenas-Sevilla et al., 2011; Uranus, 2010] and below the dew point temperature the main contribution to the interference shift is considered to be due to the adsorption of water molecules within the voids of the PCF. The adsorption on the end face mainly causes a shift in the overall power level of the interference pattern.

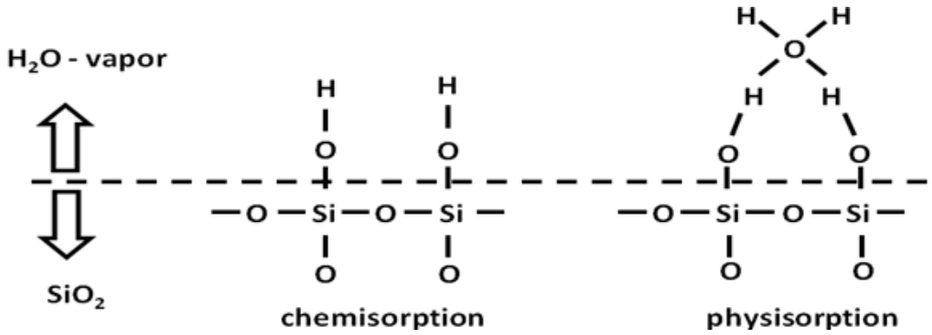

Fig. 4. Schematic representation of water vapor adsorption mechanisms on an SiO_2 surface.

3.2 Experimental characterization of the sensor

The sensor system is composed of a broadband light source (SLED), a fibre coupler/circulator (FOC), the PCF interferometer or sensor head, and an optical spectrum analyser (OSA) as shown in Fig. 5. The sensor head, as the main part of the sensor system, is composed of a small stub of PCF fusion spliced to the end of a standard SMF. The PCF in the sensor head has a microhole collapsed region near the splicing point and the free end of the PCF is exposed to ambient air. The humidity response of the device was studied at a temperature (25 ^{O}C) and at normal atmospheric pressure by placing it in a controlled environmental chamber as shown in Fig. 5. Fig. 6 shows the changes in the reflection spectrum with respect to ambient humidity for a device with L=40.5 mm. The change in the adsorption with respect to ambient humidity changes the effective refractive index of the cladding mode (n_{cl}). The resulting phase change in turn results in a shift of the interference pattern. The curves in Fig. 6 show the position of a zoomed section of the device spectrum at relative humidity values of 30, 60, 80 and 90 %RH. When humidity increases the interference pattern shifts to longer wavelengths and this shift is more significant at higher humidity values. To study the effect of reducing the length of the PCFI a second PCFI was fabricated with a shorter length of 17 mm. Fig. 7 shows the peak shift of the interferometer with respect to humidity obtained for two devices with L=17 mm and 40.5 mm.

It is observed from the Fig. 7 that the sensitivity of the device to humidity decreases as the length of the device decreases. This is due to the fact that for a small device the fibre length

available for interaction between the cladding mode with the adsorbed water vapour is less so the acquired phase difference between the interfering modes will be smaller. Hence the sensitivity to humidity change is less for a device with a smaller length of PCF. It is important to note that the shift of the interference pattern is similar to the thickness variation of the adsorbed layer of water vapour on silica i.e. increases exponentially above 60 %RH [David & Seong, 2005].

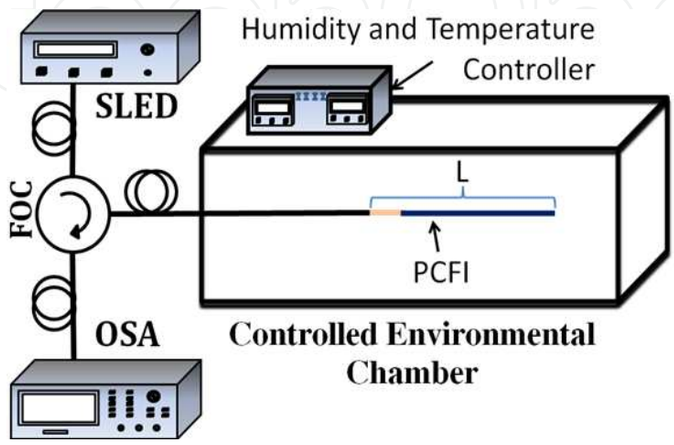

Fig. 5. Experimental arrangement for the characterisation of the PCFI with respect to relative humidity.

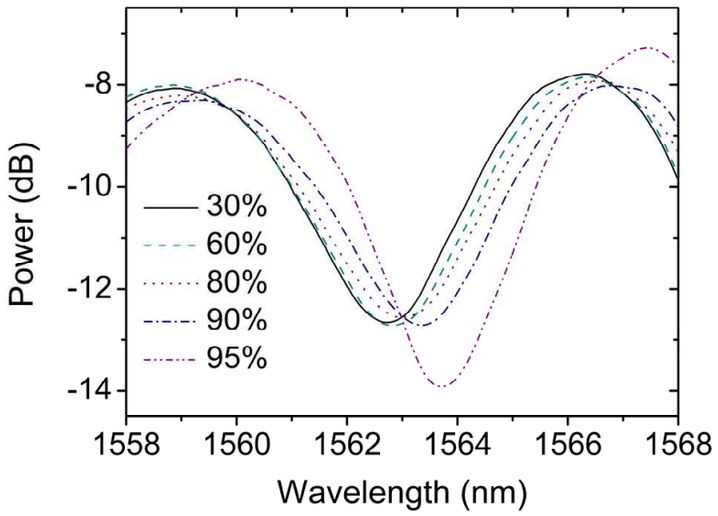

Fig. 6. Reflection spectrum of a 40.5 mm long PCFI at different humidity values.

The device sensitivity is estimated by dividing the PCFI response to humidity into three regions 27- 60 %RH, 60-80 %RH, and 80-96 %RH. The average sensitivity values observed

for the PCFI with a length of 40.5 mm in these regions are 3.7, 8.5 and 64 nm/%RH respectively and for a 17 mm long PCFI they are 1.7, 3 and 23 nm/%RH respectively. Even though the PCFI with a longer length appears more sensitive, it is likely that increasing the length of the PCFI to a much longer length is not practical because in a longer device the infiltration of water molecules may take too much time. Furthermore, since the propagation loss of the interfering cladding mode is high the fringe visibility will diminish on increasing the length of PCF. Also for a longer device the fringe spacing will be shorter which limits the measurement range of the device. Decreasing the length of the PCFI to a much shorter length is also not suitable because as seen from Fig. 2 & 3 if the length is less than 3.5 mm the fringe spacing will be greater than 100 nm, the bandwidth of a typical SLED spectrum, and therefore not suitable for observing the shift in the interference spectrum. Selecting a shorter length will also result in a reduced sensitivity but that can be improved by infiltrating the microholes with suitable hygroscopic materials. Based on our experimental observations and considering the above explained factors we suggest the best lengths for an efficient humidity sensing to be in the range from 3.5 mm to 100 mm.

The response of the PCFI to humidity variations is found to be reversible and repeatable with low hysteresis. Under laboratory conditions it is reusable, but humidity is a truly analytical measurement in which the sensor must be in direct contact with the process environment. This of course has implications of contamination and degradation of the sensor to varying degrees depending on the nature of the environment. Possible contamination agents are dust particles and chemical vapours. So a further study of the sensor head contamination in different process environments and the observation of the shift in its response in those conditions are required in order to get a better understanding of the long term stability of our sensor in field applications. In the case of a PCFI based sensor this limitation can be overcome by different ways; a recalibration of the sensor head after a certain period of time and a subsequent reuse of the sensor head during another time interval, or, since the fabrication of the PCFI based sensor head is simple and cost effective, replacing the sensor head or attaching some filters to the sensor head by which it can be protected from contamination or an ultrasonic cleaning and subsequent heating (which will remove the contaminants like dust particles without damaging the sensor head) is another method to make the sensor reusable after contamination.

A study of cross sensitivity to temperature reveals that the PCFI based humidity sensor is almost temperature independent. Conventional glass fibre relative humidity sensors require coatings and thus are always temperature dependent and, furthermore, since the majority of such sensors use polymer materials as coatings, they are not suitable for use in high-temperature applications. One significant advantage of the sensor explained here is that the sensor head is made of single material silica. This suggests that apart from low and room temperature applications the PCF interferometer based humidity sensor can also be used in harsh and high-temperature environments to monitor humidity.

4. Dew sensor based on PCFI

Dew (condensed moisture) is a problem in the fields of precision electrical devices, automobiles, air conditioning systems, warehouses and domestic equipment, etc. High humidity and condensation can create an environment where the development of mould on the wooden parts can take place and it can also cause corrosion of iron parts. This is a major

problem in the case of the works of art in the museums and churches [Camuffo & Valcher, 1986]. So there is a strong demand for a sensor able to accurately detect a high humidity or dew condensation state.

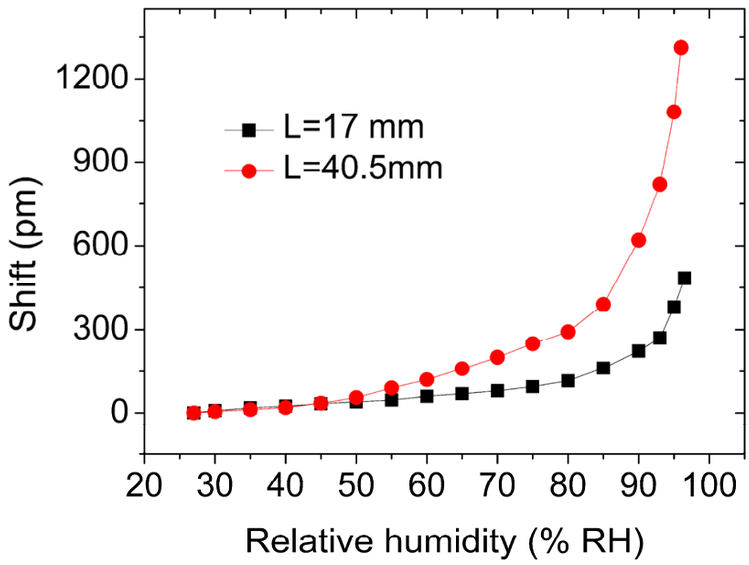

Fig. 7. Interference peak shift of the photonics crystal fibre interferometers with L= 40.5 mm and 17 mm with respect to relative humidity.

Approaches to dew detection using optical fibre have been previously reported in [Baldini et al., 2008; Kostritskii et al., 2009]. The working principle of these sensors is based on the change in the reflectivity which is observed on the surface of the fibre tip, when a water layer is formed on its distal end. The dependence on reflected power measurement scheme used in [Baldini et al., 2008; Kostritskii et al., 2009] increases the chance of measurement error due to source power fluctuations. Recently we have demonstrated a simple sensor head for dew detection based on a photonic crystal fibre interferometer (PCFI) operated in reflection mode [Mathew et al., 2011], with the advantage of good dew point measurement accuracy. The fabrication of such a sensor is very simple since it only involves cleaving and fusion splicing. Furthermore, the spectral measurement technique utilized in this work is free from errors due to source power variations. In the following section of the chapter a dew sensor based on PCFI is explained, including a study of temperature dependence of the device with different lengths of PCF. Since the sensor head is fabricated from a single material, silica, its temperature dependence is very low. From the results of the dew sensor performance with different lengths of PCF it was shown that a device with a compact length of PCF is suitable for dew sensing albeit with a reduction in the speed of response. The response of the sensor at different ambient humidity values is also included in this section.

4.1 Operating principle of the sensor

To study the response of the PCFI to dew formation it is required to set the temperature of the PCFI to dew point temperature, which is obtained from the values of ambient relative humidity and temperature. To do this let us consider a quantity of air with a constant water vapour concentration at a certain temperature, T, and relative humidity, RH < 100%. The

dew point temperature, T_d, is defined as the temperature to which this quantity of air must be cooled down such that, at a constant pressure, condensation occurs (RH = 100%). In terms of relative humidity RH and temperature T, the dew point temperature is given as:

$$T_d(T,RH) = \alpha \frac{\ln\left(\frac{RH}{100\%}\right) + \frac{\beta T}{\alpha + T}}{\beta - \ln\left(\frac{RH}{100\%}\right) - \frac{\beta T}{\alpha + T}}$$

where, α=243.12 ^{O}C and β=17.62 are the so-called Magnus parameters for the temperature range -45 to 60 ^{O}C. There fore decreasing the temperature of the PCFI increases the relative humidity close to it. At a certain stage of decreasing the temperature the relative humidity becomes 100% or reaches the dew point temperature and hence the water vapour starts to condense. The condensed water vapour on the PCFI causes a large change in the effective refractive index of the interfering cladding mode (n_{cl}) which in turn causes a large phase change between the interfering modes and therefore a large wavelength shift of the interference peaks is expected.

4.2 Experimental characterization of the sensor

The dew response of the PCF interferometer was studied by placing it on a thermoelectric cooler (TEC) as shown in Fig. 8. In order to study the influence of dew on the PCFI, it was decided to limit the PCFI length used to 42 mm or less, to suit the size of the available TEC used for temperature control. The temperature of the TEC element was controlled by a temperature controller. A thermistor was used to provide temperature feedback to the controller from the TEC element. An additional handheld thermometer was used to confirm the temperature on the TEC surface. The entire setup was placed inside a controlled environmental chamber. The inside relative humidity and the temperature of the chamber can be controlled with an accuracy of ±2 %RH and ±1 ^{O}C respectively. For the purpose of this experiment the ambient temperature inside the chamber was fixed at 25 ^{O}C.

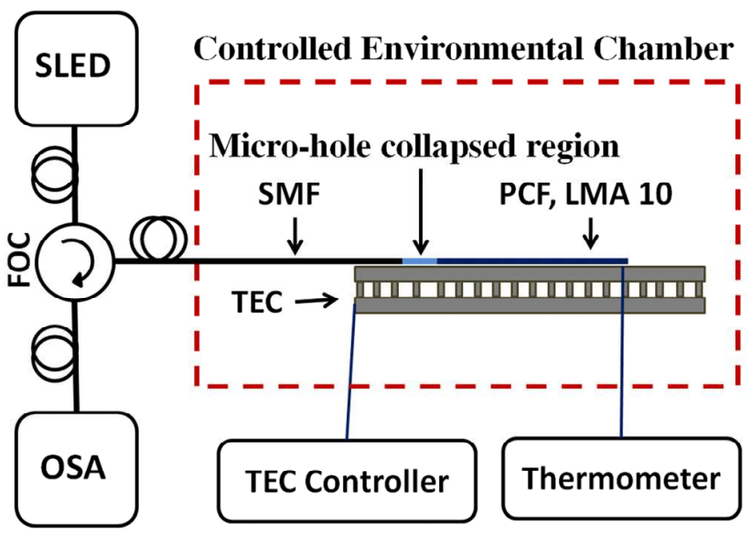

Fig. 8. Experimental arrangement for the calibration of PCFI based dew sensor.

Since the PCF is composed of only fused silica, it is expected to have minimal thermal sensitivity. The temperature dependence of the device was determined by observing the peak shift of the interference spectrum of the device for a temperature variation from 25 ^{O}C to 60 ^{O}C. The ambient humidity during the study was set to 40 % RH. When the temperature is increased from 25 ^{O}C to 60 ^{O}C the interference peak is shifted slightly to higher wavelengths. Fig. 9 shows this temperature dependence for two devices with L=17 mm and 40.5 mm. As expected the thermal sensitivity of the PCFI is very low and is further reduced for a device with the shorter length of PCF. The thermal sensitivity obtained in the experiment for a device with L= 40.5 mm is 9.5 pm/^{O}C and that for L= 17 mm is 6.2 pm/^{O}C.

The dew sensing experiments were carried out at an ambient temperature of 25 ^{O}C and at normal atmospheric pressure. To study the dew response of the device the temperature of the PCFI was decreased from ambient temperature (25 ^{O}C) to the dew point temperature at a fixed ambient relative humidity. It was found that the position of the interference peaks shifted to longer wavelengths with a decrease in temperature. This shift is similar to the humidity response of the PCFI as shown in Fig. 6 and 7. This occurs because the relative humidity inside the microholes and close to the PCFI increases with a decrease in temperature and causes a shift. At or below the dew point temperature (100% RH) water vapour condensation occurs, the condensed water vapour on the outer surface of the PCF also contributes to the change in the effective RI of the cladding mode, which results in a large spectral shift.

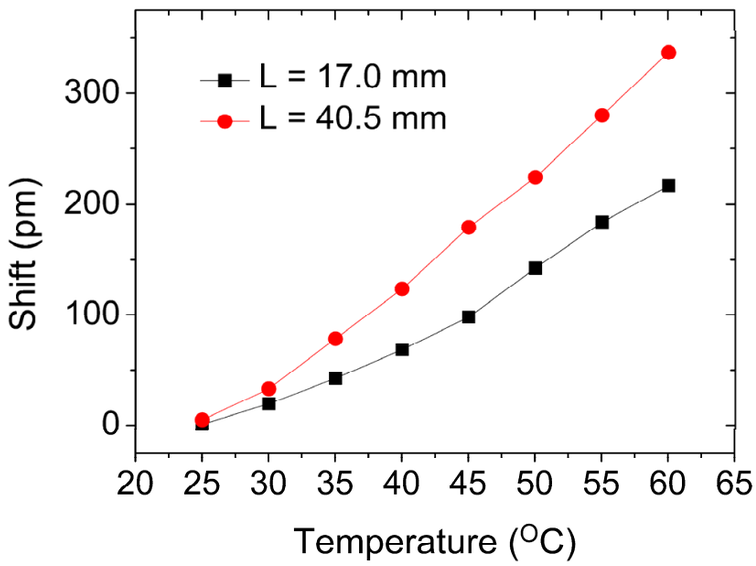

Fig. 9. Interference peak shift with respect to temperature for interferometers with PCF lengths L= 40.5 mm and 17 mm.

The spectra of two interferometers at room temperature and at the dew point temperature for devices fabricated with lengths 40.5 mm and 3.5 mm are shown in Fig. 10(a) & (b). The lengths selected are practically the largest and the smallest PCF lengths that can be studied using our experimental setup. The ambient humidity during this study was set at 60 % RH. From the Fig. 10 it is clear that relative to the period of the interferometer the shift will be larger for a longer PCFI due to a longer interaction length available for the

interference between the cladding mode and the adsorbed water vapour. Hence the sensitivity to water vapour content and thus dew point temperature is high for a device with a longer length of PCF.

It is important to note that due to the large fringe spacing it is difficult to measure the peak shift accurately for a short PCFI, therefore the comparison of sensitivities for PCFIs with different lengths is not straightforward. It should also be noted that even a PCFI with a small length (3.5 mm, fringe spacing ~90 nm) when exposed to dew point temperature for a relatively long time i.e. several minutes will result in a measurable fringe shift as shown in Fig. 10(b). This is because an increasingly thicker adsorbed water layer is formed on the silica surfaces of the PCF as time progresses. Thus compared to 3.5 mm device the ~40.5 mm device is preferable for achieving a fast response time (in the order of seconds), but when a compact length is the main requirement a shorter PCFI also can be used as a dew sensor with a reduced measurement speed. The best range of lengths suitable for dew sensing is the same as the one given above for humidity sensing.

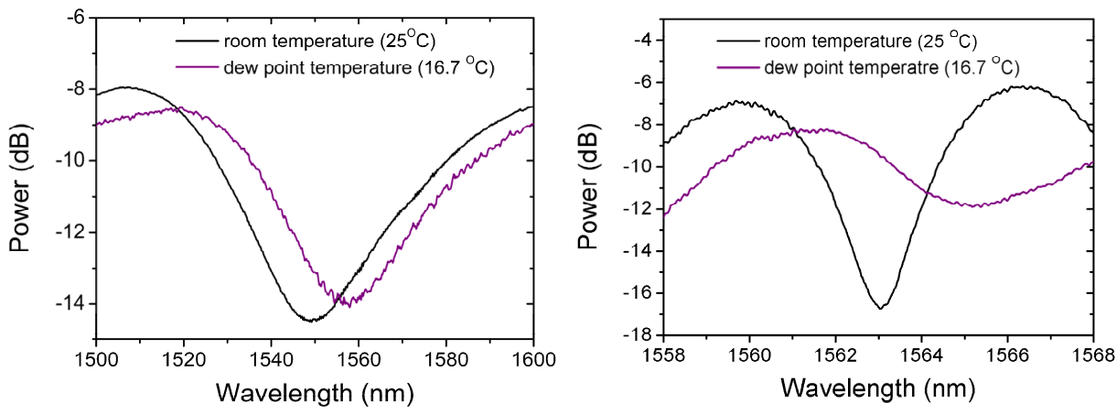

Fig. 10. (a). Interference spectra for a device with length 40.5 mm at room temperature and at dew point temperature.
(b). Interference spectra for a device with length 3.5 mm at room temperature and at dew point temperature.

The dew sensing performance of a PCFI at different environmental conditions was determined by studying the dew response of a PCFI with L= 40.5 mm at three ambient humidity values of 40, 60 and 80 %RH. At each humidity value the temperature of the PCFI is reduced from 26 ^{O}C to the corresponding dew point temperature. The peak wavelength shift of the device is plotted against temperature in Fig. 11. The three curves represent the peak shift corresponding to the ambient relative humidity values of 40, 60 and 80 %RH. The onset of the dew formation is characterized by a large shift of the interference peak which is clear in Fig. 11. The dew point temperature calculated by using equation (1) based on the corresponding ambient conditions is marked on each curve in Fig. 11. For all these three ambient humidity values the continuous spectral shift starts exactly at the dew point temperature which confirms the high dew point measurement accuracy (estimated as ±0.1 ^{O}C) of the sensor.

It is observed that at or below the dew point temperature the interference peak shifts continuously with time. This is because an increasingly thicker adsorbed water layer is formed on the silica surface of the PCF microholes as time progresses. By bringing the

temperature of the PCFI back to room temperature the interference peaks also shift back to their initial position. This shows the reversibility of the sensor. Because of the small size of the sensor head and the high sensitivity to adsorbed water vapour the demonstrated sensor response time is in seconds which is relatively fast compared to existing dew point hygrometers that take several minutes for a single measurement. The simple fabrication method, small size and the all-silica nature of the demonstrated sensor head suggest that with some simple additions such as attaching a TEC element with temperature feedback on to the PCFI, the combination can be used as a dew point hygrometer.

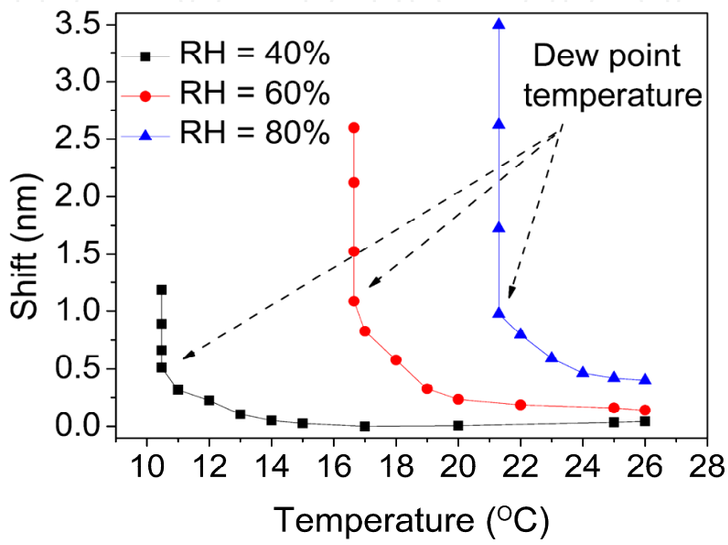

Fig. 11. Interference peak shift of PCFI with respect to temperature at three ambient humidity values of 40, 60 and 80 %RH.

5. Conclusion

A brief review of the photonic crystal fibre and the modal interferometers based on PCF are presented in this chapter. Along with the review the operating principle and the fabrication of a reflection type PCF based modal interferometer are also explained in the chapter. The dependence of the interferometer fringe spacing on the length of PCF is also explained and demonstrated experimentally. The experimental investigation and demonstration of a humidity sensor based on a PCF interferometer is presented in the chapter with a brief explanation of the operating principle of the sensor. The water vapour adsorption/desorption phenomena on silica surface are briefly addressed to explain the operating principle of the sensor. The chapter includes the experimental investigation of the relative humidity response of the sensor and the dependence of its sensitivity on the length of PCF. It is shown that a device with a longer length of the PCF section is more sensitive to relative humidity changes. A dew sensor based on PCF interferometer is presented along with the explanation of its sensing principle. The chapter presents the temperature dependence of the PCF interferometer and the dependence of its sensitivity on the length of the PCF. The dew sensing performances of PCFIs with different lengths and at different ambient relative humidity values are also presented. Based on the explained dew sensor a novel dew point hygrometer using PCF interferometer is also proposed in the chapter.

6. References

Awakuni, Y. & Calderwood, J.H. (1972). Water vapour adsorption and surface conductivity in solids. *Journal of Physics D: Applied Physics,* Vol.5, No.5, (May 1972), pp. 1038.

Baldini, F. ; Falciai, R. ; Mencaglia, A. A. ; Senesi, F. ; Camuffo, D. ; Valle, A. D. & Bergsten, C. J. (2008). Miniaturised Optical Fibre Sensor for Dew Detection Inside Organ Pipes, *Journal of Sensors*, Vol. 2008, Article ID 321065.

Barrera, D. ; Villatoro, J. ; Finazzi, V. P. ; Cardenas-Sevilla, G. A. ; Minkovich, V. P. ; Sales, S. & Pruneri, V. (2010). Low-Loss Photonic Crystal Fiber Interferometers for Sensor Networks. *Journal of Lightwave Technology*, Vol. 28, No. 24, (Dec. 2010), pp. 3542–3547.

Birks, T. A.; Knight, J. C. & Russell, P. St. J. (1997). Endlessly single-mode photonic crystal fiber, *Optics Letters*, Vol. 22, No. 13, (July 1997), pp. 961-963.

Bock, W. J.; Eftimov, T. A.; Mikulic, P. & Chen, J. (2009). An Inline Core-Cladding Intermodal Interferometer Using a Photonic Crystal Fiber, *Journal of Lightwave Technology*, Vol. 27, No. 17, (Sept. 2009), pp. 3933–3939.

Brunauer, S.; Emmett, P. H. & Teller, E. (1938). Adsorption of gases in multimolecular layers, *Journal of the American Chemical Society*, Vol.60, (February 1938), pp. 309-319.

Camuffo, D. & Valcher, S. (1986). A dew point signaller for conservation of works of art, *Environmental Monitoring and Assessment*, Vol.6, No. 2, (1986), pp. 165-170.

Cárdenas-Sevilla, G. A.; Finazzi, V. ; Villatoro, J. & Pruneri, V. (2011). Photonic crystal fiber sensor array based on modes overlapping, *Optics Express*, Vol. 19, No. 8, (April 2011), pp. 7596-7602.

Choi, H.Y. ; Kim, M. J. & Lee, B. H. (2007). All-fiber Mach-Zehnder type interferometers formed in photonic crystal fiber, *Optics Express*, Vol. 15, No. 9, (April 2007), pp. 5711–5720.

David, B. A. & Seong, H. K. (2005). Evolution of the adsorbed water layer structure on silicon oxide at room temperature, *Journal of Physical Chemistry B*, Vol. 109, No. 35, (August 2005), pp. 16760–16763.

Jha, R.; Villatoro, J. & Badenes, G. (2008). Ultrastable in reflection photonic crystal fiber modal interferometer for accurate refractive index sensing, *Applied Physics Letters*, Vol. 93, No. 19, (November 2008), pp. 191106.

Káčik, D.; Turek, I.; Martinček, I.; Canning, J.; Issa, N. & Lyytikäinen, K. (2004). Intermodal interference in a photonic crystal fibre, *Optics Express*, Vol. 12, No. 15, (July 2004), pp. 3465-3470.

Knight, J. C. (2003). Photonic crystal fibres. *Nature*, Vol. 424, No. 6950, (Aug. 2003), pp. 847–851.

Knight, J. C.; Birks, T. A.; Cregan, R. F.; Russell, P. St. J. & De Sandro, J. P. (1998). Large mode area photonic crystal fibre, *Electronics Letters*, Vol. 34, No. 13, (June 1998), pp. 1347-1348.

Knight, J. C.; Birks, T. A.; Russell, P. S. J. & Atkin, D. M. (1996). All-silica single-mode optical fiber with photonic crystal cladding. *Optics Letters*, Vol. 21, No. 19, (Oct. 1996), pp. 1547–1549.

Kostritskii, S. M.; Dikevich, A. A.; Korkishko Y. N. & Fedorov, V. A. (2009). Dew point measurement technique utilizing fiber cut reflection. *Proceedings of SPIE*, Vol. 7356, (2009), pp. 73561K.

Lim, J. H.; Jang, H. S.; Lee, K. S.; Kim, J. C. & Lee, B. H. (2004). Mach–Zehnder interferometer formed in a photonic crystal fiber based on a pair of long-period fiber gratings, *Optics Letters*, Vol. 29, No. 4, pp. 346–348.

Mathew, J.; Semenova, Y.; Rajan, G. & Farrell, G. (2010). Humidity sensor based on photonic crystal fibre interferometer, *Electronics Letters*, Vol. 46, No. 19, (September 2010), pp. 1341-1343.

Mathew, J. ; Semenova, Y. & Farrell, G. (2011). Photonic crystal fiber interferometer for dew detection, *Journal of Lightwave Technology*. DOI (identifier) 10.1109/JLT.2011.2170815.

Mathew, J. ; Semenova, Y. ; Rajan, G. & Farrell, G. (2011). Photonic crystal fiber interferometer for dew detection, *Proceedings of SPIE*, Vol. 7753, (2011), pp. 77531P.

Mathew, J.; Semenova, Y.; Rajan, G.; Wang, P. & Farrell, G. (2011). Improving the sensitivity of a humidity sensor based on fiber bend coated with a hygroscopic coating, *Optics & Laser Technology*, Vol. 43, No. 7, (October 2011) pp. 1301-1305.

Mathew, J.; Thomas, K.J.; Nampoori, V.P.N. & Radhakrishnan, P. (2007). A Comparative Study of Fiber Optic Humidity Sensors Based on Chitosan and Agarose, *Sensors & Transducers Journal*, Vol. 84, No. 10, (October 2007) pp. 1633-1640.

Monzón-Hernández, D.; Minkovich, V. P.; Villatoro, J.; Kreuzer, M. P. & Badenes, G. (2008). Photonic crystal fiber microtaper supporting two selective higher-order modes with high sensitivity to gas molecules. *Applied Physics Letters*, Vol. 93, No. 8, pp. 081106.

Renversez, G.; Kuhlmey, B. & McPhedran, R. (2003). Dispersion management with microstructured optical fibers: ultraflattened chromatic dispersion with low losses, *Optics Letters*, Vol. 28, No. 12, pp. 989-991.

Russell, P. (2003). Photonic crystal fibers. *Science*, Vol. 299, No. 5605, (January 2003), pp. 358– 362.

Russell, P. (2006). Photonic-crystal fibers. *Journal of Lightwave Technology*, Vol. 24, No. 12, (December 2006), pp. 4729–4749,.

Tiefenthaler, K. & Lukosz, W. (1985). Grating couplers as integrated optical humidity and gas sensors. *Thin Solid Films*, Vol. 126, (April 1985), pp. 205–211.

Uranus, H. P. (2010). Theoretical study on the multimodeness of a commercial endlessly single-mode PCF, *Optics Communications*, Vol. 283, No. 23, (December 2010), pp. 4649–4654.

Villatoro, J. ; Kreuzer, M. P. ; Jha, R. ; Minkovich, V. P. ; Finazzi, V. ; Badenes, G. & Pruneri, V. (2009). Photonic crystal fiber interferometer for chemical vapor detection with high sensitivity, *Optics Express*, Vol. 17, No. 3, (February. 2009), pp. 1447–1453.

Villatoro, J. ; Minkovich, V. P. ; Pruneri, V. & Badenes, G. (2007). Simple all-microstructured-optical-fiber interferometer built via fusion splicing, *Optics Express*, Vol. 15, No. 4, (February 2007), pp. 1491–1496.

Villatoro, J.; Finazzi, V.; Badenes, G. & Pruneri, V. (2009). Highly Sensitive Sensors Based on Photonic Crystal Fiber Modal Interferometers, *Journal of Sensors*, Vol. 2009, Article ID 747803, 11 pages.

Villatoro, J.; Finazzi, V.; Minkovich, V. P.; Pruneri, V. & Badenes, G. (2007). Temperature-insensitive photonic crystal fiber interferometer for absolute strain sensing, *Applied Physics Letters*, Vol. 91, No. 9, (August 2007), pp. 091109.

Voorthuyzen, J.A.; Keskin, K. & Bergveld, P. (1987). Investigations of the surface conductivity of silicon dioxide and methods to reduce it, *Surface Science,* Vol.187 No.1, (August 1987), pp. 201-211.

Yeo, T.L.; Sun, T. & Grattan, K.T.V. (2008). Fibre-optic sensor technologies for humidity and moisture measurement, *Sensors and Actuators A Physical*, Vol. 144, No. 2, (June 2008), pp. 280-295.

Zhang, C. ; Zhang, W. ; Webb, D.J. & Peng, G.D. (2010). Optical fibre temperature and humidity sensor. *Electronics Letters*, Vol. 46, No. 9, (March 2010), pp. 643-644.

Zhao, C. L.; Yang, X.; Lu, C.; Jin, W. & Demokan, M. S. (2004). Temperature-insensitive interferometer using a highly birefringent photonic crystal fiber loop mirror, *IEEE Photonics Technology Letters*, Vol. 16, No. 11, (November 2004), pp. 2535–2357.

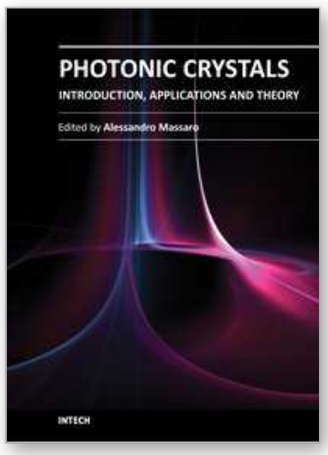

Photonic Crystals - Introduction, Applications and Theory
Edited by Dr. Alessandro Massaro

ISBN 978-953-51-0431-5
Hard cover, 344 pages
Publisher InTech
Published online 30, March, 2012
Published in print edition March, 2012

The first volume of the book concerns the introduction of photonic crystals and applications including design and modeling aspects. Photonic crystals are attractive optical materials for controlling and manipulating the flow of light. In particular, photonic crystals are of great interest for both fundamental and applied research, and the two dimensional ones are beginning to find commercial applications such as optical logic devices, micro electro-mechanical systems (MEMS), sensors. The first commercial products involving two-dimensionally periodic photonic crystals are already available in the form of photonic-crystal fibers, which use a microscale structure to confine light with radically different characteristics compared to conventional optical fiber for applications in nonlinear devices and guiding wavelengths. The goal of the first volume is to provide an overview about the listed issues.

How to reference
In order to correctly reference this scholarly work, feel free to copy and paste the following:

Jinesh Mathew, Yuliya Semenova and Gerald Farrell (2012). Photonic Crystal Fibre Interferometer for Humidity Sensing, Photonic Crystals - Introduction, Applications and Theory, Dr. Alessandro Massaro (Ed.), ISBN: 978-953-51-0431-5, InTech, Available from: http://www.intechopen.com/books/photonic-crystals-introduction-applications-and-theory/photonic-crystal-fiber-interferometer-for-humidity-sensing

INTECH
open science | open minds

InTech Europe
University Campus STeP Ri
Slavka Krautzeka 83/A
51000 Rijeka, Croatia
Phone: +385 (51) 770 447
Fax: +385 (51) 686 166
www.intechopen.com

InTech China
Unit 405, Office Block, Hotel Equatorial Shanghai
No.65, Yan An Road (West), Shanghai, 200040, China
中国上海市延安西路65号上海国际贵都大饭店办公楼405单元
Phone: +86-21-62489820
Fax: +86-21-62489821

IntechOpen